FUDMA Journal of Sciences (FJS)
ISSN online: 2616-1370
ISSN print: 2645 - 2944
Vol. 10 No. 21, November, 2026, pp 65 – 78
DOI: https://doi.org/10.33003/fjs-2026-1021-6312

Optimization of Glyphosate Removal from Aqueous Solution Using Shea Nut Shell Bioadsorbent: A Response Surface Methodology Approach

Muhammad Sani Abdullahi and Okunola J. Oluwole

Chemistry Department. Federal University Dutsin-Ma. Katsina State, Nigeria.

*Corresponding authors' email: msani7543@gmail.com

Received: 14 Aug. 2026
Accepted: 22 Oct. 2026
Published: 05 Nov. 2026

ABSTRACT

Glyphosate contamination of water resources from agricultural activities presents a significant environmental challenge, particularly in Nigeria where the herbicide is widely used. This study evaluated a shea nut shell (Vitellaria paradoxa)-derived bioadsorbent for glyphosate removal from aqueous solution and assessed the principal adsorption variables using response surface methodology based on a Box-Behnken design. The bioadsorbent was prepared by alkaline (NaOH) treatment followed by carbonization at 400 °C for 2 h and characterized using FTIR, SEM-EDS, PXRD, and XRF. Characterization revealed lignocellulosic functional groups (C-H, C=C, C-O-C, C-O), a rough and porous surface morphology, semi-crystalline cellulose with a crystallite size of 15.69 nm, and inorganic constituents including potassium, calcium, and iron. The point of zero charge (PZC) was 6.8. Batch adsorption experiments were conducted using a 46-run Box-Behnken design investigating pH (2–10), contact time (10–180 min), adsorbent dosage (0.10–2.00 g/100 mL), initial glyphosate concentration (10–100 mg/L), and temperature (25–45 °C). Experimental glyphosate removal ranged from 0% to 100%, with complete removal observed in two runs, while the highest experimental adsorption capacity was 62.14 mg/g. The quadratic response surface model explained 52.92% of variation (R^2 = 0.5292) but exhibited limited predictive capability (adjusted R^2 = 0.1526; predicted R^2 = −0.8186), and the overall model was not statistically significant (F = 1.405, p = 0.2085). Initial glyphosate concentration was the only statistically significant linear factor (F = 6.106, p = 0.0206), with a significant quadratic effect (F = 7.187, p = 0.0128). The contact time × adsorbent dosage interaction approached significance (p = 0.0544). These findings demonstrate the potential of shea nut shell as a low-cost bioadsorbent for glyphosate removal; however, the conditions of maximum removal are reported as best-performing conditions within the experimental region rather than statistically validated optimum conditions, and independent validation is required.

Keywords: Glyphosate, Bioadsorbent, Shea Nut Shell, Response Surface Methodology, Box-Behnken Design, Adsorption

INTRODUCTION

Water pollution from agricultural activities is a major environmental concern because pesticides applied to farmland can enter surface water and groundwater through runoff, erosion, and leaching. Among these pesticides, glyphosate is widely used for weed control due to its broad-spectrum herbicidal activity, and its extensive application has raised concerns about its occurrence in soil and aquatic environments (Ighalo et al., 2021; Kimbi Yaah et al., 2024). Glyphosate, chemically known as N-(phosphonomethyl) glycine, is a systemic and non-selective herbicide that inhibits 5-enolpyruvylshikimate-3-phosphate synthase (EPSPS), an enzyme involved in the shikimate pathway of susceptible plants. Glyphosate is highly polar and water-soluble and contains phosphonate, carboxyl, and amino functional groups. These ionizable groups influence its behaviour in aqueous environments and enable interactions with suitable adsorbent surfaces (Sen, 2021; Ighalo et al., 2021).

The use and occurrence of glyphosate are relevant to Nigeria, where herbicides are increasingly used for agricultural weed management. Glyphosate has been reported among commonly used herbicides by farmers in Southwestern Nigeria, while residues have also been detected in surface water and groundwater associated with agricultural activities (Ayoola et al., 2023; Olaniyi et al., 2025). Specifically, glyphosate was reported to be used by 81.9% of farmers surveyed across Ogun, Ondo, and Oyo States (Olaniyi et al., 2025), and concentrations reaching 29.40 ± 0.83 mg/L were detected in wet-season surface water in Oyo State (Ayoola et al., 2023). Its occurrence in water therefore creates a need for effective and affordable treatment methods.

Different methods are available for removing glyphosate from water, including membrane separation, advanced oxidation, biological treatment, electrochemical processes, and adsorption (Kimbi Yaah et al., 2024). Among these methods, adsorption is attractive because of its relatively simple operation and potential application using low-cost adsorbent materials. Agricultural wastes have received attention as potential bioadsorbents because they are renewable, inexpensive, and predominantly lignocellulosic. Their cellulose, hemicellulose, and lignin structures contain functional groups that may interact with contaminants in aqueous systems. Converting these wastes into adsorbents also provides an opportunity for agricultural-waste valorization (Liu et al., 2022). Several studies have demonstrated the effectiveness of agricultural waste-derived adsorbents for glyphosate removal, including biochars from rice husk, coffee husk, and woody biomass (Herath et al., 2016; Mayakaduwa et al., 2016; Lam et al., 2023), as well as clay-biochar composites (Rallet et al., 2022). However, the

performance of these materials varies considerably depending on feedstock, preparation conditions, and solution chemistry, underscoring the need for continued evaluation of locally available feedstocks.

Shea nut shell is an agricultural residue generated during the processing of shea nuts. As a lignocellulosic material, it has potential for conversion into a bioadsorbent. The use of shea nut shell for water treatment could therefore provide a low-cost adsorbent while creating a beneficial use for an agricultural residue (Duwiejuah et al., 2018). However, despite the potential of agricultural wastes as adsorbents, information on the specific use of shea nut shell for glyphosate removal from aqueous solution remains limited. In particular, there is a need to establish its adsorption performance and determine the influence of important operational variables. Response Surface Methodology (RSM) provides a statistical approach for evaluating the individual and combined effects of process variables and determining optimum operating conditions. The Box-Behnken design can be applied to investigate selected adsorption variables efficiently and develop a predictive model for glyphosate removal. Therefore, this study evaluates shea nut shell-derived bioadsorbent for the removal of glyphosate from aqueous solution through adsorbent characterization, adsorption studies, and response surface modelling using RSM based on the Box-Behnken experimental design

Aim: This study aims to evaluate shea nut shell-derived bioadsorbent for glyphosate removal from aqueous solution and assess the principal adsorption variable using response surface methodology based on a Box–Behnken design.

MATERIALS AND METHODS

Materials

Shea nut shells were collected, washed, dried, and ground. All chemicals and reagents used were of analytical grade. Sodium hydroxide (NaOH) and hydrochloric acid (HCl) were used for pH adjustment and adsorbent preparation. Distilled water was used throughout.

Preparation of Shea Nut Shell Bioadsorbent

Shea nut shells were pretreated by soaking in 0.1 M NaOH for 24 hours, washed until neutral, dried at 105 °C for 24 h, and carbonized in a muffle furnace at 400 °C for 2 h under limited-air conditions. The carbonized material was cooled to room temperature, ground, and sieved to a particle size of < 250 µm. This alkaline treatment enhances surface porosity and removes lignin or hemicellulose (Igbemi et al., 2021).

Characterization of Bioadsorbent

The prepared bioadsorbent was characterized using Fourier-transform infrared spectroscopy (FTIR), scanning electron microscopy coupled with energy-dispersive X-ray spectroscopy (SEM-EDS), powder X-ray diffraction (PXRD), and X-ray fluorescence (XRF). The point of zero charge (PZC) was determined by the salt addition method: 0.1 g of bioadsorbent was added to 50 mL of 0.1 M NaCl solutions adjusted to initial pH values between 2 and 12, shaken for 24 h, and the final pH was measured; the PZC was taken as the pH at which $\Delta pH = 0$

FTIR: Functional groups were identified by recording spectra over a suitable wavenumber range.

SEM-EDS: Surface morphology and elemental composition were examined at different magnifications.

PXRD: Powder X-ray diffraction analysis was used to investigate the structural characteristics of the prepared shea nut shell bioadsorbents.

Approximately 10 mg of each dried sample was finely ground and evenly distributed on the XRD sample holder. The diffraction patterns were recorded using Cu Kα radiation with a wavelength (λ) of 1.5406 Å over a 2θ range of 5–50°.

The resulting diffractograms were examined for broad and sharp diffraction features associated with the amorphous and crystalline components of the prepared materials. The positions and relative intensities of the major diffraction peaks were compared to assess structural differences among the prepared adsorbents.

The relationship between the X-ray wavelength, diffraction angle and interplanar spacing was described using Bragg's law:

$n\lambda = 2d \sin \theta$

Where:

n = order of diffraction

λ = wavelength of the incident X-ray radiation

d = interplanar spacing

θ = Bragg diffraction angle

For first-order diffraction, where n = 1, the interplanar spacing was calculated as: $d = \lambda / (2 \sin \theta)$

Where crystalline-phase identification was undertaken, the observed diffraction peaks were compared with appropriate reference patterns in the International Centre for Diffraction Data Powder Diffraction File (ICDD-PDF) database.

Where crystallite-size determination was applicable, the average crystallite size was calculated using the Scherrer equation:

$D = K\lambda / (\beta \cos \theta)$

Where:

D = average crystallite size (nm)

K = Scherrer shape factor, approximately 0.9

λ = wavelength of Cu Kα radiation (0.15406 nm)

β = full width at half maximum (FWHM) of the selected diffraction peak in radians

θ = Bragg angle of the selected diffraction peak

The Scherrer calculation was applicable only to sufficiently defined crystalline diffraction peaks for which the required peak-width information was available.

The exact scan step size and counting time should be reported from the original XRD instrument output or analytical report.

XRF: Inorganic elemental composition was determined.

Preparation of Glyphosate Solutions

Synthetic aqueous solutions of glyphosate were prepared in the laboratory at concentrations specified by the experimental design.

Batch Adsorption Experiments

Batch adsorption experiments were performed in 250 mL conical flasks containing 100 mL of glyphosate solution of the required initial concentration. The required amount of bioadsorbent (0.10–2.00 g/100 mL) was added, and the pH was adjusted to the desired value (2–10) using 0.1 M HCl or 0.1 M NaOH. The flasks were sealed and agitated in a thermostatic shaker at 150 rpm for the specified contact time (10–180 min) and temperature (25–45 °C) according to the Box-Behnken experimental matrix. After adsorption, the adsorbent was separated by filtration through a 0.45 µm membrane filter, and the residual glyphosate concentration was determined using UV-Visible spectrophotometry at 296 nm. All experiments were performed in triplicate, and the mean values were used for analysis. The limit of detection (LOD) of the spectrophotometric method, calculated as 3.3 × (standard deviation of the blank)/(slope of the calibration curve), was 0.28 mg/L.

Box–Behnken Response Surface Methodology Design

A Box–Behnken design (BBD) consisting of 46 experimental runs was employed to investigate five independent variables: pH (2–10), contact time (10–180 min), adsorbent dosage (0.10–2.00 g/100 mL), initial glyphosate concentration (10–100 mg/L), and temperature (25–45 °C). The design included six centre-point runs to assess experimental reproducibility and estimate pure error.

Calculation of Adsorption Responses

The initial glyphosate concentration (C_0) and equilibrium or residual concentration (C_e) were used to calculate the percentage removal and equilibrium adsorption capacity.

Percentage Glyphosate Removal

Removal (%) = $[(C_0 - C_e)/C_0] \times 100$

Where: C_0 = initial glyphosate concentration (mg/L); C_e = residual or equilibrium glyphosate concentration (mg/L).

Equilibrium Adsorption Capacity

$q_e = [(C_0 - C_e)V]/m$

Where: q_e = equilibrium adsorption capacity (mg/g); C_0 = initial glyphosate concentration (mg/L); C_e = equilibrium glyphosate concentration (mg/L); V = volume of glyphosate solution (L); m = mass of adsorbent used (g).

Since 100 mL of glyphosate solution was used in each experiment: V = 100 mL = 0.100 L. Therefore:

$q_e = [(C_0 - C_e) \times 0.100]/m$

The percentage removal and adsorption capacity obtained from the experimental runs were used as response variables for evaluating the effects of the operational parameters and for subsequent statistical modelling using RSM.

Statistical Analysis

Experimental data were analyzed using Design-Expert software. Analysis of variance (ANOVA) was used to evaluate the significance of model terms. Model adequacy was assessed using R^2, adjusted R^2, predicted R^2, lack-of-fit tests, and diagnostic plots**.**

RESULTS AND DISCUSSION

Characterization of Shea Nut Shell Bioadsorbent

FTIR Analysis

The FTIR spectrum of the shea nut shell (Vitellaria paradoxa) bioadsorbent revealed characteristic absorption bands corresponding to the major lignocellulosic constituents of the biomass (Figure 1). The peaks observed at 2922.2 and 2847.7 cm^{-1} were assigned to asymmetric and symmetric stretching vibrations of aliphatic C-H groups, indicating the presence of cellulose, hemicellulose, and lignin. The absorption band at 1565.5 cm^{-1} was attributed to C=C aromatic ring stretching of lignin, while the bands at 1371.7 and 1155.4 cm^{-1} were assigned to C-O-C and C-O stretching vibrations, respectively, characteristic of polysaccharides. The broad band around 2340.8 cm^{-1} was attributed to O-H stretching of adsorbed water or phenolic groups. The presence of these oxygen-containing functional groups is expected to facilitate glyphosate adsorption through hydrogen bonding and electrostatic interactions.

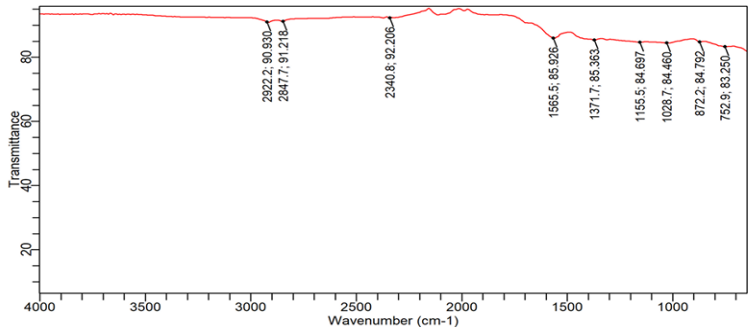


Figure 1: FTIR Analysis of Sheanut Shell Bio-Adsorbent

Scanning Electron Microscopy (SEM)

Scanning electron microscopy (SEM) was used to examine the surface morphology of the shea nut shell (*Vitellaria paradoxa*) bio-adsorbent at magnifications of 500×, 1000×, and 2000×. The micrographs revealed irregularly shaped particles with rough and heterogeneous surfaces containing cracks, grooves, and fractured edges. At higher magnifications, the biomass exhibited a fibrous lignocellulosic structure with interconnected pores, longitudinal channels, and numerous surface cavities. These morphological features are characteristic of plant-derived adsorbents and provide a large effective surface area together with multiple active sites for adsorption. The interconnected pore network facilitates the diffusion of adsorbate molecules into the adsorbent matrix, thereby enhancing adsorption efficiency. Bright particulate deposits observed on the surface are attributed to inorganic mineral constituents or residual ash and may further contribute to surface heterogeneity. The SEM observations confirm that the prepared sheanut shell bio-adsorbent possesses a porous and structurally stable morphology suitable for the adsorption of glyphosate from aqueous solutions.

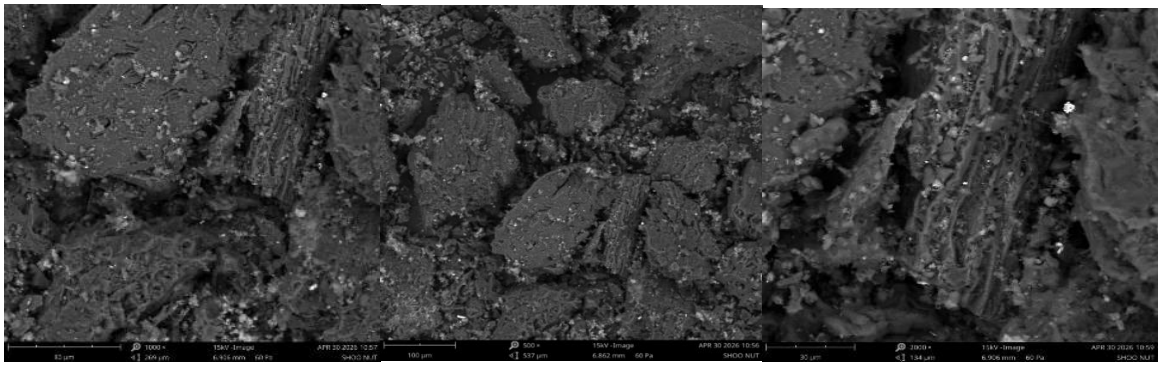


Figure 2: SEM Analysis of Sheanut Shell bio-Adsorbent

Scanning Electron Microscopy (SEM) -Energy-dispersive X-ray Analysis of Sheanut Shell Bio-Adsorbent

The SEM and EDS analyses collectively demonstrate that the prepared shea nut shell (*Vitellaria paradoxa*) bio-adsorbent possesses both favourable morphological and chemical characteristics required for efficient adsorption. SEM analysis revealed a rough, heterogeneous, and porous surface containing irregular particles, cracks, grooves, fissures, and inter-particle voids that increase the available surface area and facilitate the diffusion of glyphosate molecules into the adsorbent. EDS analysis confirmed that the adsorbent is predominantly composed of carbon and oxygen, together with trace mineral elements including magnesium, aluminium, phosphorus, potassium, calcium, titanium, vanadium, manganese, and iron. The abundance of oxygen-containing functional groups and naturally occurring mineral constituents provides multiple active sites for adsorption through hydrogen bonding, electrostatic attraction, ion exchange, surface complexation, and physical adsorption. Therefore, the combined SEM and EDS results demonstrate that the sheanut shell bio-adsorbent possesses a porous morphology and chemically active surface suitable for the effective removal of glyphosate and other contaminants from aqueous media.

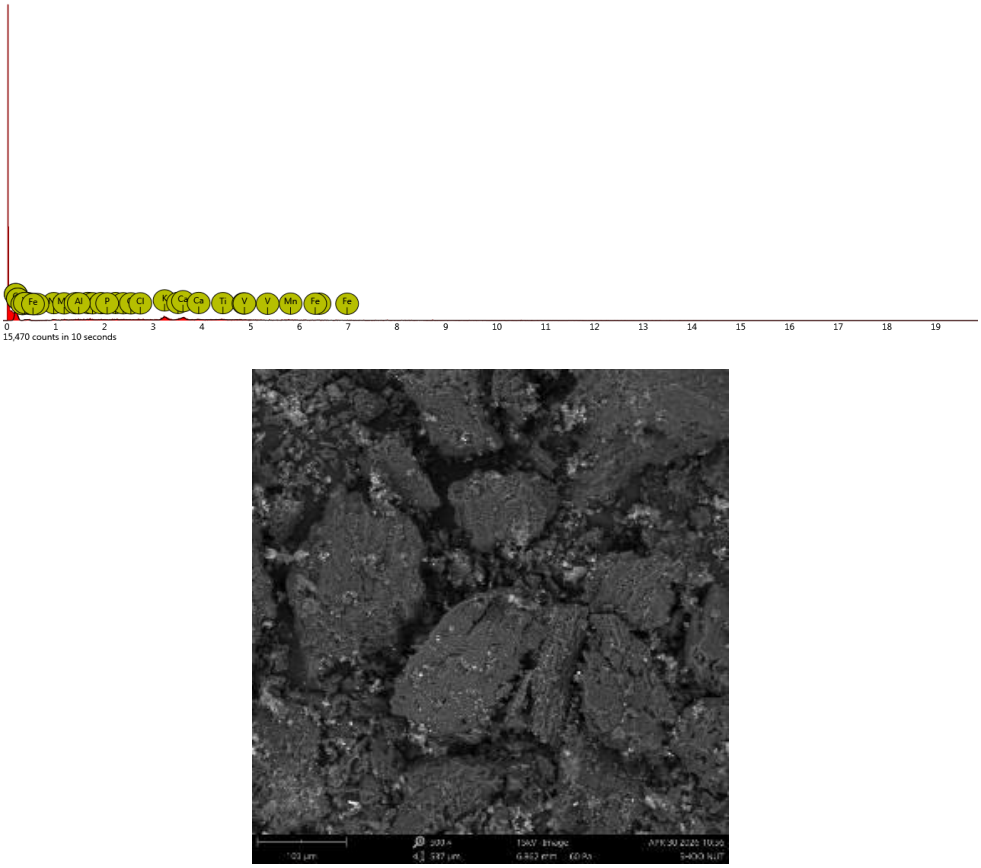


Figure 3: Scanning Electron Microscopy (SEM) - Energy-Dispersive X-ray Analysis of Sheanut Shell Bio-Adsorbent

X-ray Diffraction (XRD) Analysis of Sheanut Shell (Vitellaria Paradoxa) Bio-Adsorbent

The XRD analysis of the sheanut shell (*Vitellaria paradoxa*) bio-adsorbent revealed a dominant diffraction peak at 2θ = 24.6939° with a relative intensity of 100% and a d-spacing of 3.60238 Å.This peak is attributed to the semi-crystalline cellulose fraction present within the lignocellulosic structure of the biomass. The relatively low peak height (69.19 counts) and broad peak width (FWHM = 0.5184°) indicate a low degree of crystallinity and the predominance of an amorphous phase. The broadening of the diffraction peak suggests structural disorder within the cellulose matrix and limited crystal growth. The calculated crystallite size of 15.69 nm further confirms the presence of nanoscale crystalline domains dispersed within an amorphous lignin–hemicellulose matrix. Such a small crystallite size is characteristic of agricultural biomass and indicates a large proportion of surface atoms and grain boundaries. These features enhance the accessibility of adsorption sites and promote interaction between the adsorbent and pollutant molecules. The XRD peak parameters and crystallite size data demonstrate that the sheanut shell bio-adsorbent possesses a predominantly amorphous lignocellulosic structure with minor semi-crystalline cellulose regions. The low crystallinity, broad diffraction peak, and nanoscale crystallite size are favourable characteristics for adsorption because they provide increased surface heterogeneity, greater accessibility of functional groups, and improved adsorption capacity for contaminants such as glyphosate.

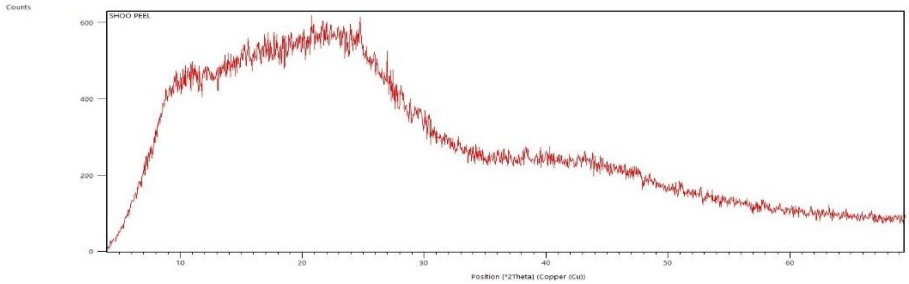


Figure 4: X-Ray Diffraction (XRD) Analysis of Sheanut Shell Bio-Adsorbent

Table 1: XRD Characteristics of Sheanut Shell Bio-Adsorbent

Peak No.	2θ (°)	I (cts)	Rel. Int. (%)	FWHM (°)	β (rad)	d (Å)	D (nm)	Phase
1	24.6939	69.19	100.00	0.5184	0.00905	3.60238	15.69	Semi-crystalline cellulose

Key: 2θ = Diffraction Angle; θ = Bragg Angle; I = Peak Intensity; Rel. Int. = Relative Intensity; FWHM = Full Width at Half Maximum; β = FWHM in Radians; d = Interplanar Spacing; D = Crystallite Size; K = Scherrer Shape Factor; λ = X-Ray Wavelength; cts = Counts; Å = Ångström; nm = Nanometre.

X-ray Fluorescence (XRF) of Sheanut Shell Bio-adsorbent

The XRF spectrum of the sheanut shell (*Vitellaria paradoxa*) bio-adsorbent revealed the presence of several inorganic elements, indicating that the biomass contains naturally occurring mineral constituents. The detected elements include carbon (C), potassium (K), calcium (Ca), barium (Ba), cerium (Ce), iron (Fe), nickel (Ni), copper (Cu), zinc (Zn), and strontium (Sr). Among the detected elements, strontium (Sr) exhibited the most intense characteristic peak, indicating that it is the predominant detectable inorganic element in the sample. Moderate peaks corresponding to potassium (K) and calcium (Ca) were also observed, suggesting that these elements are naturally present in appreciable amounts within the sheanut shell. The occurrence of potassium and calcium is consistent with their roles as essential plant nutrients and common constituents of lignocellulosic biomass. Trace amounts of iron (Fe), nickel (Ni), copper (Cu), zinc (Zn), barium (Ba), and cerium (Ce) were also detected. These elements may originate from natural mineral uptake during plant growth, soil-derived impurities, or residual inorganic ash remaining after sample preparation. Although present in relatively low concentrations, these mineral constituents can influence the surface chemistry of the bio-adsorbent and may contribute to adsorption through ion exchange, electrostatic interactions, or surface complexation. The XRF results demonstrate that the sheanut shell bio-adsorbent contains a diverse range of naturally occurring inorganic elements. The presence of alkali and alkaline earth metals, particularly potassium and calcium, together with trace transition metals, may enhance the adsorption properties of the bio-adsorbent by providing additional active sites for interaction with glyphosate and other contaminants.

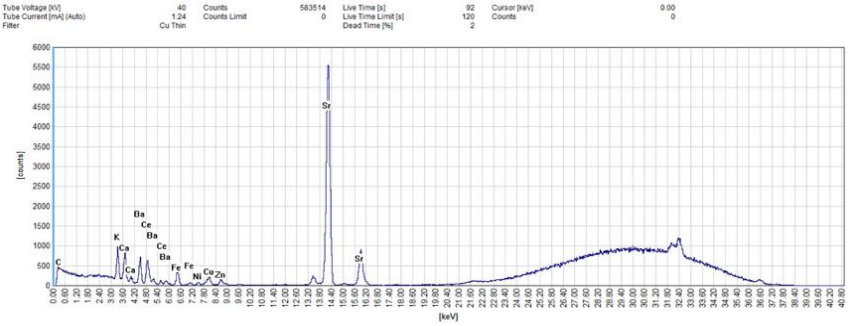


Figure 5: X-ray Fluorescence (XRF) of Sheanut Shell Bio-adsorbent

Point of Zero Charge (PZC)

The point of zero charge of the shea nut shell bioadsorbent was determined to be pH 6.8 (Figure 5). At solution pH values below the PZC, the adsorbent surface carries a net positive charge, whereas above the PZC the surface is net negatively charged. Since glyphosate exists predominantly as a monoanion ($pKa_1 = 2.0$, $pKa_2 = 2.6$) and dianion ($pKa_3 = 5.6$) over the pH range studied, electrostatic attraction between the negatively charged glyphosate species and the positively charged adsorbent surface is expected to be favourable at pH < 6.8, while repulsion may occur at pH > 6.8. This behaviour is consistent with the general trend of decreasing removal with increasing pH observed in the present study.

Adsorption Study and Optimization of Glyphosate Removal

Calibration Curve of Glyphosate34

Figure 6. presents the calibration curve of glyphosate obtained by plotting the absorbance of standard solutions (20–100 mg/L) against their corresponding concentrations at 296 nm. The calibration curve exhibited an excellent linear relationship, described by the regression equation A = 0.0119C + 0.0061, with a coefficient of determination (R^2 = 1.000), indicating perfect linearity within the concentration range studied. The positive slope demonstrates that absorbance increased proportionally with increasing glyphosate concentration, while the small intercept indicates negligible background interference from the blank solution. The excellent linearity confirms the reliability and accuracy of the UV–Visible spectrophotometric method for glyphosate quantification. The calibration equation was subsequently used to determine the equilibrium concentration (Ce) of glyphosate remaining after adsorption, from which the adsorption capacity (Qe) and percentage removal (%) were calculated for all experimental runs.

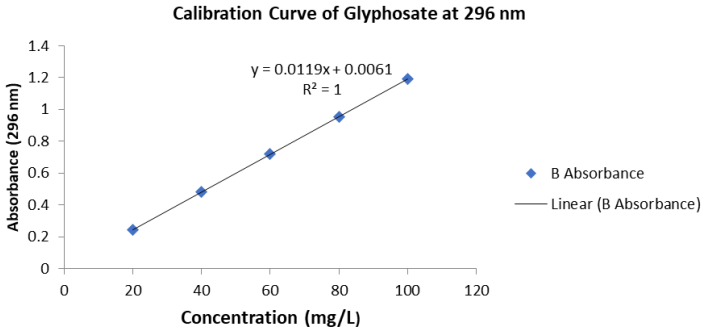


Figure 6: Calibration Curve of Glyphosate

Experimental Design Matrix and Experimental Responses for Glyphosate Adsorption

Table presents the Box–Behnken experimental design matrix and the corresponding adsorption responses obtained for glyphosate removal using the shea nut shell-derived adsorbent. The design comprised 46 experimental runs, in which five independent variables pH (2–10), contact time (10–180 min), adsorbent dosage (0.10–2.00 g/100 mL), initial glyphosate concentration (10–100 mg/L), and temperature (25–45 °C) were systematically varied to evaluate their effects on the adsorption process. The experimental responses measured for each run included the equilibrium concentration (Ce, mg/L), adsorption capacity (Qe, mg/g), and percentage removal (%). The results showed considerable variation among the experimental runs, with Ce ranging from 0.00 to 100.00 mg/L, Qe ranging from 0.00 to 62.14 mg/g, and glyphosate removal efficiency ranging from 0.00 to 100.00%, demonstrating the significant influence of the operating variables on adsorption performance. These experimental data served as the basis for developing the response surface models, evaluating the significance of the process variables and their interactions, and determining the optimum operating conditions for maximum glyphosate removal.

Table 2: Experimental Design Matrix and Experimental Responses for Glyphosate Adsorption

Std	Run	pH	Contact Time (min)	Adsorbent Dosage (g/100 mL)	Initial Conc. (mg/L)	Temp (°C)	Ce (mg/L)	Qe (mg/g)	Removal (%)
1	1	2	10	1.05	55	35	18.59	3.47	66.20
2	2	10	10	1.05	55	35	32.53	2.14	40.85
3	3	2	180	1.05	55	35	0.00	5.24	100.00
4	4	10	180	1.05	55	35	34.08	1.99	38.04
5	5	6	95	0.10	10	35	9.95	0.50	0.50
6	6	6	95	2.00	10	35	1.00	4.50	90.00
7	7	6	95	0.10	100	35	37.86	62.14	62.14
8	8	6	95	2.00	100	35	37.06	3.15	62.94
9	9	6	10	1.05	55	25	41.41	1.29	24.71
10	10	6	180	1.05	55	25	11.05	4.19	79.91
11	11	6	10	1.05	55	45	29.48	2.43	46.40
12	12	6	180	1.05	55	45	25.30	2.83	54.00
13	13	2	95	0.10	55	35	24.26	30.74	55.89

Std	Run	pH	Contact Time (min)	Adsorbent Dosage (g/100 mL)	Initial Conc. (mg/L)	Temp (°C)	Ce (mg/L)	Qe (mg/g)	Removal (%)
14	14	10	95	0.10	55	35	25.81	29.19	53.07
15	15	2	95	2.00	55	35	48.70	0.32	11.45
16	16	10	95	2.00	55	35	53.85	0.06	2.09
17	17	6	95	1.05	10	25	9.80	0.19	2.00
18	18	6	95	1.05	100	25	56.45	4.15	43.55
19	19	6	95	1.05	10	45	9.60	0.38	4.00
20	20	6	95	1.05	100	45	21.71	7.46	78.29
21	21	6	10	0.10	55	35	28.30	26.70	48.55
22	22	6	180	0.10	55	35	51.10	3.90	7.09
23	23	6	10	2.00	55	35	50.61	0.22	7.98
24	24	6	180	2.00	55	35	3.95	2.55	92.82
25	25	6	180	1.05	10	35	9.30	0.67	7.03
26	26	10	95	1.05	10	35	9.70	0.29	3.00
27	27	2	95	1.05	100	35	90.16	0.94	9.84
28	28	10	95	1.05	100	35	100.00	0.00	0.00
29	29	6	95	0.10	55	25	5.75	49.25	89.55
30	30	6	95	2.00	55	25	4.63	2.52	91.58
31	31	6	95	0.10	55	45	51.63	3.37	6.13
32	32	6	95	2.00	55	45	4.49	2.53	91.84
33	33	2	95	1.05	55	25	25.88	2.77	52.95
34	34	10	95	1.05	55	25	1.27	5.12	97.69
35	35	2	95	1.05	55	45	13.89	3.92	74.75
36	36	10	95	1.05	55	45	17.06	3.61	68.98
37	37	6	10	1.05	10	35	9.87	0.12	1.26
38	38	6	180	1.05	10	35	9.30	0.67	7.03
39	39	6	10	1.05	100	35	15.57	8.04	84.43
40	40	6	180	1.05	100	35	17.13	7.89	82.87
41	41	6	95	1.05	55	35	24.62	2.89	55.24
42	42	6	95	1.05	55	35	15.87	3.73	71.15
43	43	6	95	1.05	55	35	18.36	3.49	66.62
44	44	6	95	1.05	55	35	0.00	5.24	100.00
45	45	6	95	1.05	55	35	23.88	2.96	56.58
46	46	6	95	1.05	55	35	16.70	3.65	69.64

Description of Model Selection and ANOVA for the Quadratic Model

The model selection and adequacy statistics identified the quadratic model as the most appropriate response surface model for describing glyphosate removal because it was the highest-order polynomial that was not aliased. Although the sequential model sum of squares showed that the quadratic model was not statistically significant ($p = 0.1354$), it was recommended by Design-Expert for further analysis. The model summary statistics indicated that the quadratic model explained 52.92% of the variation in glyphosate removal ($R^2 = 0.5292$). However, the relatively low adjusted R^2 (0.1526) and negative predicted R^2 (−0.8186) suggest that the model has limited predictive capability beyond the experimental data. The lack-of-fit test produced an F-value of 4.417 with a p-value of 0.0533, indicating that the lack of fit was not statistically significant relative to the pure error, and therefore the model adequately represented the experimental data within the investigated design space.

The analysis of variance (ANOVA) further evaluated the effects of the process variables on glyphosate removal. The overall quadratic model produced an F-value of 1.405 and a p-value of 0.2085, indicating that the model was not statistically significant relative to the experimental noise. Among the linear factors, only the initial glyphosate concentration (Factor D) had a statistically significant effect on glyphosate removal ($F = 6.106$, $p = 0.0206$), whereas pH (A), contact time (B), adsorbent dosage (C), and temperature (E) did not significantly influence the response ($p > 0.05$). None of the two-factor interaction terms were statistically significant, although the interaction between contact time and adsorbent dosage (BC) approached significance ($F = 4.074$, $p = 0.0544$), suggesting a possible combined influence on the adsorption process. Among the quadratic terms, only the quadratic effect of initial glyphosate concentration (D^2) was significant ($F = 7.187$, $p = 0.0128$), indicating that glyphosate removal exhibited a significant curvature with respect to the initial concentration. The remaining quadratic terms (A^2, B^2, C^2, and E^2) were not statistically significant.

Overall, these findings indicate that initial glyphosate concentration was the most influential factor governing glyphosate removal, while the effects of pH, contact time, adsorbent dosage, temperature, and their interactions were comparatively less pronounced within the experimental region. The non-significant overall model and the negative predicted R^2 are important limitations that constrain the use of the model for predictive optimization; consequently, the model is used here primarily for interpreting response-surface behaviour and for identifying best-performing conditions rather than for statistically validated optimization.

Table 3: Model Selection and Adequacy Statistics for Percentage Removal (%)

Model	Sequential F-value	Sequential p-value	Lack-of-Fit F-value	Lack-of-Fit p-value	Std.Dev.	R^2	Adjusted R^2	Predicted R^2	PRESS	Decision
Linear	1.630	0.1742	4.563	0.0481	32.854	0.1693	0.0655	-0.1164	58,023.713	Not Selected
2FI	0.852	0.5855	4.931	0.0417	33.481	0.3530	0.0294	-0.6506	85,785.973	Not Selected
Quadratic	1.872	0.1354	4.417	0.0533	31.285	0.5292	0.1526	-0.8186	94,522.242	Suggested/ Selected
Cubic	0.903	0.5840	6.927	0.0267	32.235	0.8001	0.1004	-10.2172	583,003.410	Aliased

Table 4: ANOVA for Quadratic Model of Removal

Source	Sum of Squares	df	Mean Square	F-value	p-value	
Model	27504.67	20	1375.23	1.41	0.2085	not significant
A-PH	345.87	1	345.87	0.3534	0.5576	
B-TIME	1249.27	1	1249.27	1.28	0.2693	
C-DOSAGE	1020.48	1	1020.48	1.04	0.3170	
D-INITIAL CONCENTRATION	5976.84	1	5976.84	6.11	0.0206	
E-TEMPERATURE	207.00	1	207.00	0.2115	0.6496	
AB	335.07	1	335.07	0.3423	0.5637	
AC	10.69	1	10.69	0.0109	0.9176	
AD	8.44	1	8.44	0.0086	0.9268	
AE	637.82	1	637.82	0.6516	0.4271	
BC	3987.92	1	3987.92	4.07	0.0544	
BD	13.43	1	13.43	0.0137	0.9077	
BE	566.44	1	566.44	0.5787	0.4539	
CD	1966.92	1	1966.92	2.01	0.1687	
CE	1750.59	1	1750.59	1.79	0.1931	
DE	267.98	1	267.98	0.2738	0.6054	
A^2	2370.00	1	2370.00	2.42	0.1323	
B^2	575.43	1	575.43	0.5879	0.4504	
C^2	680.46	1	680.46	0.6952	0.4123	
D^2	7034.94	1	7034.94	7.19	0.0128	
E^2	43.37	1	43.37	0.0443	0.8350	
Residual	24469.43	25	978.78			
Lack of Fit	23158.70	20	1157.93	4.42	0.0533	not significant
Pure Error	1310.73	5	262.15			
Core Total	51974.10	45				

Final Quadratic Regression Equation for Glyphosate Removal (%)

The quadratic regression equation describes the relationship between pH (A), contact time (B), adsorbent dosage (C), initial glyphosate concentration (D), temperature (E) and the percentage removal of glyphosate. In the linear terms, pH and temperature have negative coefficients (−4.6494 and −3.5969, respectively), indicating that increasing these factors individually tends to decrease glyphosate removal within the experimental region. In contrast, contact time, adsorbent dosage and initial glyphosate concentration have positive coefficients (+8.8363, +7.9863 and +19.3275, respectively), indicating positive linear effects on removal. Among the interaction terms, the time × dosage interaction (BC) has the largest positive coefficient (+31.5750), suggesting that the combined effect of contact time and adsorbent dosage can enhance removal. Conversely, the dosage × initial concentration interaction (CD) has a relatively large negative coefficient (−22.1750), indicating an antagonistic combined effect. The negative quadratic coefficients for pH, contact time, dosage and especially initial concentration (D^2 = −28.3917) indicate curvature in their relationships with glyphosate removal, with the strongest curvature associated with initial concentration. The positive coefficient for temperature squared (E^2 = +2.2292) indicates a comparatively weak upward curvature. Overall, the equation indicates that initial glyphosate concentration has the strongest linear and quadratic influence among the individual factors, which is consistent with the ANOVA results showing that D and D^2 were significant model terms.

Removal (%) = 69.8717 - 4.6494A + 8.8363B + 7.9863C + 19.3275D - 3.5969E - 9.1525AB - 1.6350AC - 1.4525AD - 12.6275AE + 31.5750BC - 1.8325BD - 11.9000BE - 22.1750CD + 20.9200CE + 8.1850DE - 16.4792A^2 - 8.1200B^2 - 8.8300C^2 - 28.3917D^2 + 2.2292E^2

Diagnostic Evaluation of the Quadratic Response Surface Model

The diagnostic plots were examined to evaluate the statistical adequacy of the quadratic response surface model developed for the removal of glyphosate using the sheanut shell bio-adsorbent and to assess the underlying assumptions of the regression analysis. The normal probability plot of residuals showed that the majority of the experimental observations followed the theoretical reference line reasonably closely, particularly within the central region of the distribution,

indicating that the residuals were approximately normally distributed. Some departures from the reference line were observed at both the lower and upper tails, suggesting minor deviations from normality and the presence of some observations with relatively larger standardized residuals; however, the overall distribution did not exhibit a pronounced systematic departure that would indicate severe non-normality.

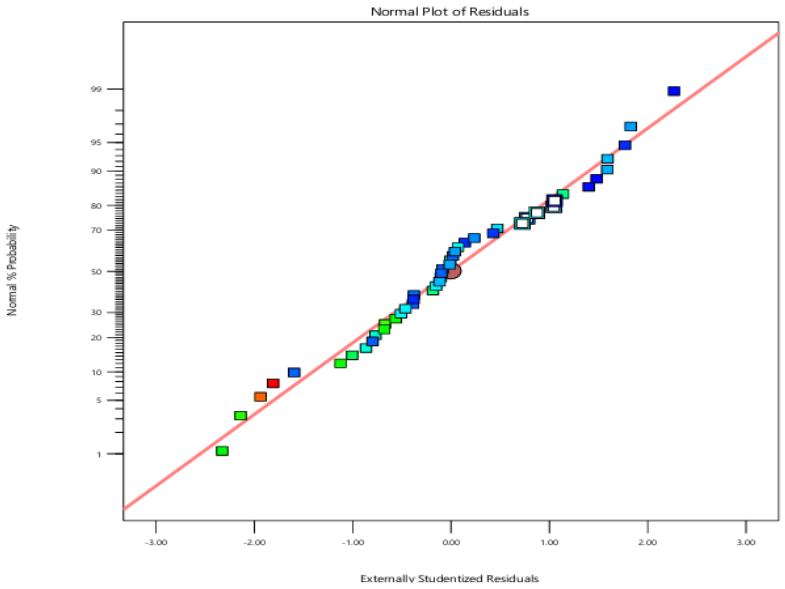


Figure 7: Normal Probability Plot of Residuals

The residuals versus predicted values plot showed that the residuals were distributed on both sides of the zero-reference region over the range of predicted glyphosate removal values, with no clearly defined curvature, progressive trend, or pronounced funnel-shaped distribution. This pattern provides reasonable evidence that the model did not exhibit a strong systematic bias in its predictions and that substantial heteroscedasticity was not visually apparent, although the relatively wide dispersion of some residuals indicates that a considerable proportion of experimental variability remained unexplained by the fitted model.

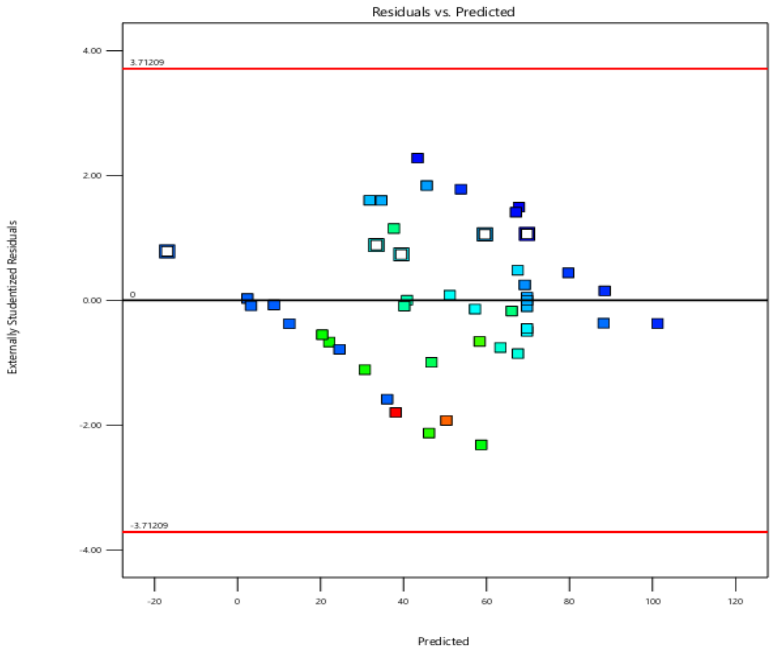


Figure 8: Residuals Versus Predicted Values

The residuals versus experimental run plot further showed that the residuals were distributed across the sequence of experimental runs without a consistent increasing, decreasing, or cyclic pattern. The absence of a discernible run-order trend suggests that there was no obvious systematic drift in the experimental error with run sequence and provides reasonable support for the assumption that the residuals were not strongly dependent on experimental order. Nevertheless, individual runs with comparatively large positive or negative residuals indicate that certain experimental conditions produced

responses that differed substantially from those predicted by the model and should be interpreted as sources of unexplained variation rather than automatically regarded as experimental errors.

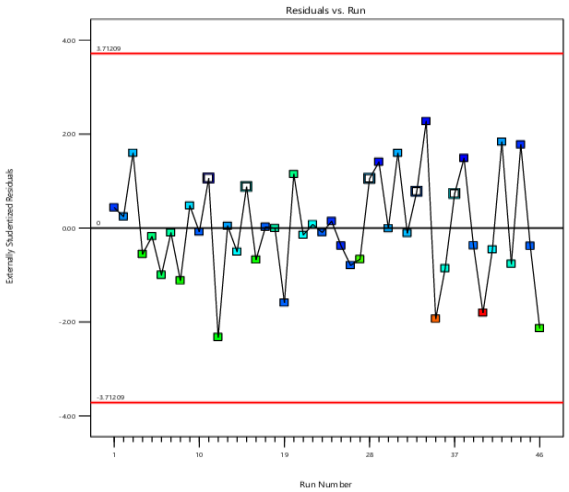


Figure 9: Residuals Versus Experimental Run

The predicted versus actual values plot demonstrated a general positive association between the experimentally measured and model-predicted glyphosate removal percentages, indicating that the fitted quadratic model captured part of the variation in the response across the experimental domain. However, the observations were not tightly concentrated around the ideal prediction line, with appreciable deviations occurring for several experimental runs, demonstrating limited agreement between predicted and observed values for some combinations of pH, contact time, adsorbent dosage, initial glyphosate concentration, and temperature. This observation is consistent with the model summary statistics, particularly the R^2 value of 0.5292, which indicates that approximately 52.92% of the observed variability in glyphosate removal was accounted for by the quadratic model, while the relatively low adjusted R^2 of 0.1526 indicates that the explanatory performance of the model was substantially reduced after adjustment for the number of fitted terms. More importantly, the predicted R^2 of −0.8186 indicates poor predictive capability of the fitted model for predicting responses through the model's prediction-error framework. Thus, although the diagnostic plots do not reveal a severe or obvious violation of the principal residual assumptions, they also do not support describing the model as having strong predictive accuracy.

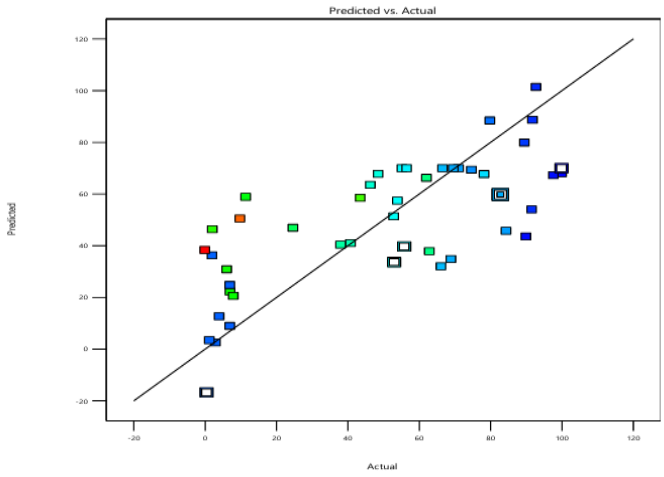


Figure 10: Predicted Versus Actual Values

The diagnostic assessment therefore indicates that the quadratic model provides a reasonable statistical description of certain response patterns within the investigated experimental region, but substantial unexplained variability remains. This interpretation should be considered alongside the non-significant overall quadratic model ($F = 1.405$, $p = 0.2085$) and the significant effects of initial glyphosate concentration (D; $p = 0.0206$) and its quadratic term (D^2; $p = 0.0128$). Consequently, the diagnostic results support cautious use of the quadratic model for interpretation of the response-surface behavior and visualization of factor effects, while its relatively weak predictive statistics indicate that optimization results should subsequently be subjected to experimental validation before being considered reliable for practical application.

3D Response Surface Analysis of Glyphosate Removal

The four three-dimensional response surface plots collectively illustrate the effects of pH, contact time, adsorbent dosage, initial glyphosate concentration, and temperature on glyphosate removal efficiency within the experimental design space. The surfaces demonstrate that glyphosate removal varied considerably with changes in the operating conditions, with the response exhibiting curved and non-linear patterns across several factor combinations. The pH × dosage surface showed variation in removal across the investigated pH and dosage levels, although their interaction was not statistically significant ($p = 0.9176$). Similarly, the time × dosage surface demonstrated a more pronounced change in the response, and this interaction approached statistical significance ($F = 4.074$, $p = 0.0544$), suggesting that the influence of adsorbent dosage may vary with contact time, although the interaction did not reach the conventional 5% significance level. The time × temperature surface showed changes in predicted removal across the investigated conditions, but their interaction was not statistically significant ($p = 0.4539$). The initial concentration × dosage surface showed substantial variation in removal, reflecting the important contribution of initial glyphosate concentration to the adsorption response; however, their specific interaction was also not statistically significant ($p = 0.1687$). Overall, the response surfaces demonstrate that the adsorption process is influenced by the simultaneous variation of the experimental factors, with initial glyphosate concentration representing the most statistically important linear factor ($p = 0.0206$) and its quadratic term also significant ($p = 0.0128$). Therefore, the 3D surfaces provide useful graphical visualization of the response behavior and help identify regions of relatively higher and lower predicted glyphosate removal, while the statistical significance of individual effects and interactions should be interpreted primarily from the ANOVA results.

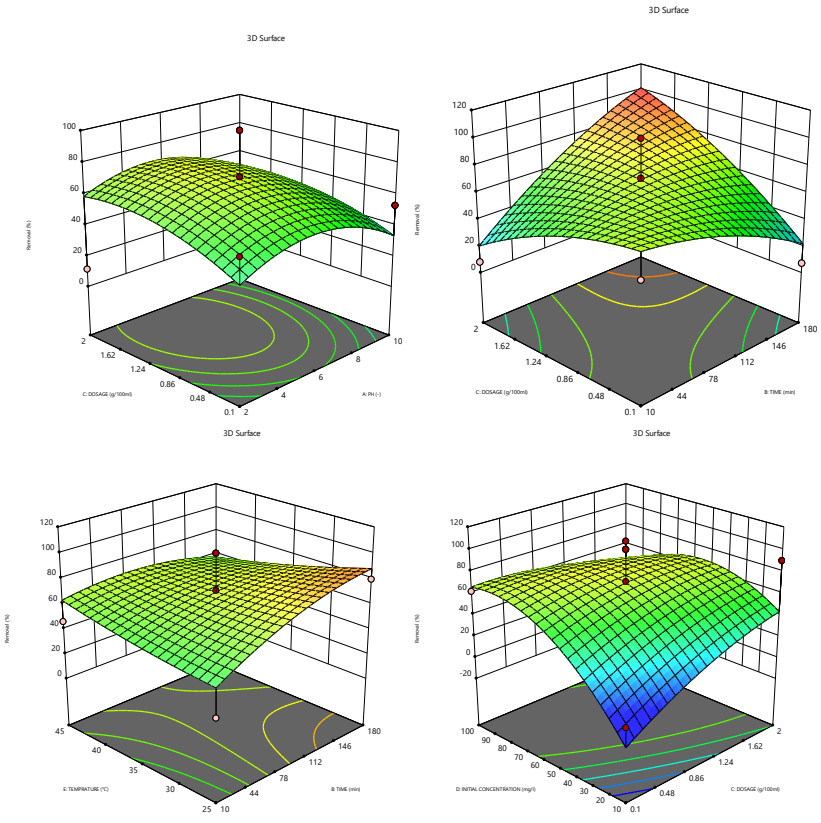


Figure 11: 3D Plot for the Statistical Analysis

Combined Interpretation of the Four Contour Plots

The contour plots collectively illustrate the combined effects of pH, contact time, adsorbent dosage, temperature, and initial glyphosate concentration on glyphosate removal efficiency. The pH × dosage plot shows that the predicted removal was generally higher around the intermediate pH region and intermediate-to-high adsorbent dosage, although the corresponding interaction was not statistically significant (AC, $p = 0.9176$). The contact time × dosage plot indicates an overall tendency for removal to increase toward longer contact times and higher adsorbent dosage, with the highest predicted response occurring in the upper region of the design space; notably, this interaction approached statistical significance (BC, $p = 0.0544$). The contact time × temperature contour indicates that higher removal was generally predicted at longer contact times, particularly around the lower-to-moderate temperature range, whereas the time × temperature interaction was not statistically significant (BE, $p = 0.4539$). Among the four plots, the initial concentration × dosage response showed the clearest gradient, with removal increasing substantially as the initial glyphosate concentration increased, particularly toward approximately 60–100 mg/L. This observation agrees with the ANOVA, which identified initial glyphosate concentration (D) as a significant linear factor ($p = 0.0206$) and its quadratic term (D^2) as significant ($p = 0.0128$). Overall, the contour plots demonstrate that the response varied across the experimental design space, with initial glyphosate concentration emerging as the most influential factor, while the contact time–dosage combination showed a potentially meaningful trend. Nevertheless, because

the overall quadratic model was not statistically significant ($p = 0.2085$), the contour plots should be interpreted primarily as visual representations of predicted response patterns rather than definitive evidence of statistically significant interactions.

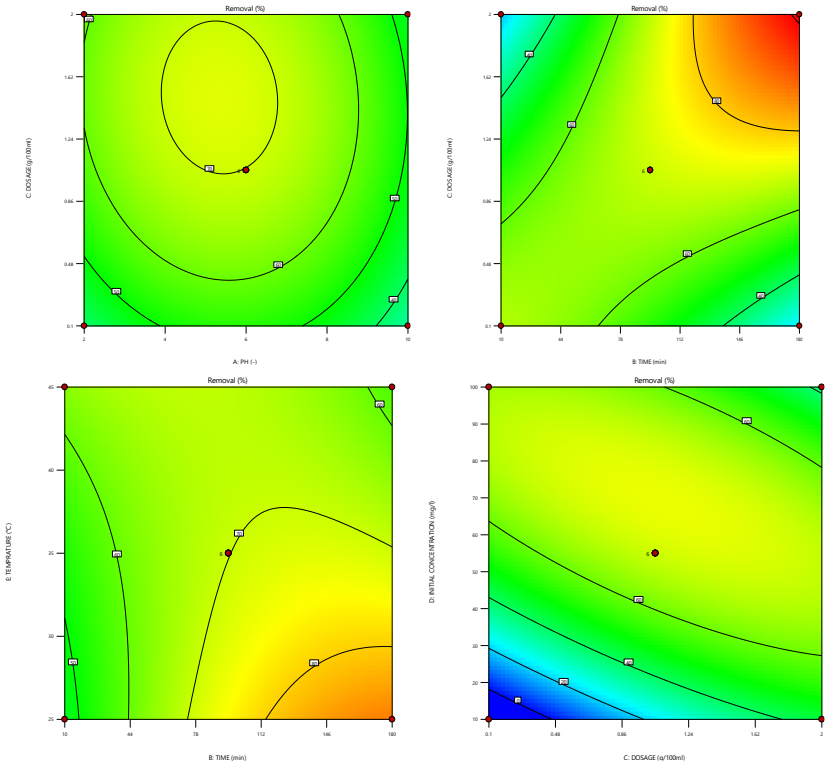


Figure 11: Contour Plots

Discussion of Adsorption Mechanisms and Comparison with Literature

The adsorption of glyphosate onto the shea nut shell bioadsorbent is expected to proceed through multiple mechanisms, consistent with the heterogeneous, oxygen-rich, and mineral-containing surface revealed by characterization. FTIR analysis confirmed the presence of C-H, C=C, C-O-C, and C-O functional groups, while EDS and XRF identified oxygen and mineral constituents (K, Ca, Fe, and others). These features provide several possible glyphosate–surface interactions: (i) hydrogen bonding between the phosphonate and carboxyl groups of glyphosate and surface hydroxyl/carboxyl groups; (ii) electrostatic attraction between the negatively charged glyphosate anion and positively charged surface sites at pH < PZC (6.8); (iii) ligand exchange and surface complexation involving mineral oxides (e.g., Fe, Al); and (iv) ion exchange with surface-associated cations (K^+, Ca^{2+}). The decrease in removal with increasing pH observed in the present study is consistent with the PZC of 6.8 and the speciation of glyphosate, which becomes increasingly negatively charged as pH rises above its pKa values (2.0, 2.6, and 5.6), leading to electrostatic repulsion at alkaline pH.

The maximum experimental adsorption capacity of 62.14 mg/g obtained in this study is comparable to or higher than several agricultural waste-derived adsorbents reported in the literature. For example, Mayakaduwa et al. (2016) reported glyphosate adsorption capacities of approximately 30–45 mg/g for woody biochars, while Herath et al. (2016) reported capacities in the range of 20–40 mg/g for rice husk biochar. Lam et al. (2023) reported glyphosate removal by Fe_3O_4-loaded coffee husk biochar with capacities up to approximately 50 mg/g. The relatively high capacity observed here may be attributed to the alkaline pretreatment, which removes lignin and hemicellulose and exposes cellulose hydroxyl groups, as well as to the naturally occurring mineral content (K, Ca, Fe) that can participate in surface complexation. Nevertheless, direct comparison is complicated by differences in feedstock, pyrolysis conditions, solution chemistry, and the range of initial concentrations tested, and the present results should therefore be regarded as indicative of the potential of shea nut shell rather than as a definitive performance benchmark.

The significant effect of initial glyphosate concentration ($p = 0.0206$) and its quadratic term ($p = 0.0128$) indicates that the driving force for adsorption increases with concentration, as expected from mass-transfer considerations, but that the response exhibits curvature consistent with saturation of available binding sites at higher concentrations. The approaching-significant time × dosage interaction ($p = 0.0544$) suggests that higher dosage shortens the time required to approach equilibrium, which is consistent with increased availability of active sites. The weak and non-significant effects of pH, temperature, and other interactions within the experimental region may reflect the narrow range of conditions and the dominant influence of concentration, as well as the heterogeneity of the adsorbent surface, which may buffer the effects of individual variables. These interpretations should be treated cautiously given the non-significant overall model and limited predictive statistics.

CONCLUSION

This study successfully prepared and characterized a shea nut shell (Vitellaria paradoxa)-derived bioadsorbent and evaluated its potential for glyphosate removal from aqueous solution using Response Surface Methodology based on a Box–Behnken design. Characterization confirmed a porous,

heterogeneous lignocellulosic structure with oxygen-containing functional groups, semi-crystalline cellulose (crystallite size 15.69 nm), and mineral constituents. Batch adsorption experiments yielded glyphosate removal ranging from 0% to 100%, with complete removal observed in two runs and a maximum experimental adsorption capacity of 62.14 mg/g. The quadratic response surface model explained 52.92% of variation (R^2 = 0.5292) but exhibited limited predictive capability (adjusted R^2 = 0.1526; predicted R^2 = −0.8186), and the overall model was not statistically significant (F = 1.405, p = 0.2085). Initial glyphosate concentration was the only significant linear factor (p = 0.0206), with a significant quadratic effect (p = 0.0128), while the contact time × adsorbent dosage interaction approached significance (p = 0.0544). These findings demonstrate that shea nut shell possesses potential as a low-cost bioadsorbent for glyphosate removal; however, the conditions associated with maximum removal should be regarded as best-performing conditions within the experimental region rather than statistically validated optimum conditions. The study was limited to synthetic aqueous solutions under controlled laboratory conditions, and independent validation experiments were not conducted. Future work should therefore include equilibrium isotherm and kinetic modelling, thermodynamic parameter determination, validation using real contaminated water matrices, regeneration and reuse testing, competing-ion studies, BET surface area analysis, post-adsorption characterization, and techno-economic assessment before field-scale application.

REFERENCES

Ahuja, M., Kumar, L., Kumar, K., Shingatgeri, V. M., & Kumar, S. (2024). Glyphosate: A review on its widespread prevalence and occurrence across various systems. *Environmental Science: Advances*, *3*, 1030–1038. https://doi.org/10.1039/D4VA00085D

Ayoola, R. T., Olujimi, O. O., Bada, B. S., & Dedeke, G. A. (2023). Seasonal variations in the levels of glyphosate in soil, water and crops from three farm settlements in Oyo State, Nigeria. *Heliyon*, *9*(9), e20324. https://doi.org/10.1016/j.heliyon.2023.e20324

Bhatnagar, A., Sillanpää, M., & Witek-Krowiak, A. (2015). Agricultural waste peels as versatile biomass for water purification: A review. *Chemical Engineering Journal*, *270*, 244–271.

Borggaard, O. K., & Gimsing, A. L. (2008). Fate of glyphosate in soil and the possibility of leaching to ground and surface waters: A review. *Pest Management Science*, *64*(4), 441–456. https://doi.org/10.1002/ps.1512

Cicilinski, A. D., Melo, V. F., & Peralta-Zamora, P. G. (2025). Glyphosate and AMPA sorption onto synthetic iron (oxyhydr)oxides: A comparative study. *Journal of Molecular Liquids*, *426*, 127303. https://doi.org/10.1016/j.molliq.2025.127303

Dai, Y., Sun, Q., Wang, W., Lü, L., Liu, M., Li, J., Yang, S., Sun, Y., Zhang, K., Xu, J., Zheng, W., Hu, Z., Yang, Y., Gao, Y., Chen, Y., Zhang, X., Gao, F., & Zhang, Y. (2018). Utilizations of agricultural waste as adsorbent for the removal of contaminants: A review. *Chemosphere*, *211*, 235–253. https://doi.org/10.1016/j.chemosphere.2018.06.179

Dissanayake Herath, G. A., Poh, L. S., & Ng, W. J. (2019). Statistical optimization of glyphosate adsorption by biochar and activated carbon with response surface methodology. *Chemosphere*, *227*, 533–540. https://doi.org/10.1016/j.chemosphere.2019.04.078

Duke, S. O., & Powles, S. B. (2008). Glyphosate: A once-in-a-century herbicide. *Pest Management Science*, *64*(4), 319–325.

Duwiejuah, A. B., Cobbina, S. J., Quainoo, A. K., Abubakari, A. H., & Bakobie, N. (2018). Adsorption of potentially toxic metals from mono and multi-metal systems using groundnut and shea nut shell biochars. *Journal of Health & Pollution*, *8*(18), 180602. https://doi.org/10.5696/2156-9614-8.18.16

Food and Agriculture Organization of the United Nations & World Health Organization. (2016). *Pesticide residues in food 2016: Special session of the Joint FAO/WHO Meeting on Pesticide Residues*. Food and Agriculture Organization of the United Nations.

Foo, K. Y., & Hameed, B. H. (2010). Insights into the modeling of adsorption isotherm systems. *Chemical Engineering Journal*, *156*(1), 2–10.

Georgin, J., Franco, D. S. P., Ramos, C. G., Tran, H. N., Benettayeb, A., Imanova, G., & Ali, I. (2024). Recent advances in removing glyphosate herbicide and its aminomethylphosphonic acid metabolite in water. *Journal of Molecular Liquids*, 124786. https://doi.org/10.1016/j.molliq.2024.124786

Hall, K. E., Spokas, K. A., Gámiz, B., Cox, L., Papiernik, S. K., & Koskinen, W. C. (2018). Glyphosate sorption/desorption on biochars—Interactions of physical and chemical processes. *Pest Management Science*, *74*(5), 1206–1212. https://doi.org/10.1002/ps.4530

Herath, I., Kumarathilaka, P., Al-Wabel, M. I., Abduljabbar, A., Ahmad, M., Usman, A. R. A., & Vithanage, M. (2016). Mechanistic modeling of glyphosate interaction with rice husk derived engineered biochar. *Microporous and Mesoporous Materials*, *225*, 280–288. https://doi.org/10.1016/j.micromeso.2016.01.017

Herviyanti, Maulana, A., Lita, A. L., Prasetyo, T. B., Monikasari, M., & Ryswaldi, R. (2022). Characteristics of Inceptisol ameliorated with rice husk biochar to glyphosate adsorption. *Sains Tanah: Journal of Soil Science and Agroclimatology*, *19*(2), 230–240. https://doi.org/10.20961/stjssa.v19i2.61614

Hu, Y. S., Zhao, Y. Q., & Sorohan, B. (2011). Removal of glyphosate from aqueous environment by adsorption using water industrial residual. *Desalination*, *271*(1–3), 150–156.

Ighalo, J. O., Ajala, O. J., Adeniyi, A. G., Babatunde, E. O., & Ajala, M. A. (2021). Ecotoxicology of glyphosate and recent advances in its mitigation by adsorption. *Environmental Science and Pollution Research*, *28*(3), 2655–2668. https://doi.org/10.1007/s11356-020-11521-5

International Agency for Research on Cancer. (2017). *Some organophosphate insecticides and herbicides*. IARC Monographs on the Evaluation of Carcinogenic Risks to

Humans (Vol. 112). International Agency for Research on Cancer.

Kanissery, R., Gairhe, B., Kadyampakeni, D., Batuman, O., & Alferez, F. (2019). Glyphosate: Its environmental persistence and impact on crop health and nutrition. *Plants*, *8*(11), 499.

Kimbi Yaah, V. B., Ahmadi, S., Quimbayo M., J., Morales-Torres, S., & Ojala, S. (2024). Recent technologies for glyphosate removal from aqueous environment: A critical review. *Environmental Research*, *240*, 117477. https://doi.org/10.1016/j.envres.2023.117477

Lita, A. L., Hidayat, E., Mohamad Sarbani, N. M., Harada, H., Yonemura, S., Mitoma, Y., Herviyanti, & Gusmini. (2023). Glyphosate removal from water using biochar based coffee husk loaded Fe_3O_4. *Water*, *15*(16), 2945. https://doi.org/10.3390/w15162945

Liu, G., Dai, Z., Liu, X., Dahlgren, R. A., & Xu, J. (2022). Modification of agricultural wastes to improve sorption capacities for pollutant removal from water—A review. *Carbon Research*, *1*, 24. https://doi.org/10.1007/s44246-022-00025-1

Mayakaduwa, S. S., Kumarathilaka, P., Herath, I., Ahmad, M., Al-Wabel, M., Ok, Y. S., Usman, A., Abduljabbar, A., & Vithanage, M. (2016). Equilibrium and kinetic mechanisms of woody biochar on aqueous glyphosate removal. *Chemosphere*, *144*, 2516–2521. https://doi.org/10.1016/j.chemosphere.2015.07.080

Mesnage, R., Benbrook, C., & Antoniou, M. N. (2019). Insight into the confusion over surfactant co-formulants in glyphosate-based herbicides. *Food and Chemical Toxicology*, *128*, 137–145.

Mo, J., Yang, Q., Zhang, N., Zhang, W., Zheng, Y., & Zhang, Z. (2018). A review on agro-industrial waste (AIW) derived adsorbents for water and wastewater treatment. *Journal of Environmental Management*, *227*, 395–405. https://doi.org/10.1016/j.jenvman.2018.08.069

Mohan, D., Sarswat, A., Ok, Y. S., & Pittman, C. U., Jr. (2014). Organic and inorganic contaminants removal from water with biochar, a renewable, low-cost and sustainable adsorbent—A critical review. *Bioresource Technology*, *160*, 191–202.

Olaniyi O.O., et al. (2025). (Full citation details to be verified and completed).

Rallet, D., Paltahe, A., Tsamo, C., & Loura, B. (2022). Synthesis of clay-biochar composite for glyphosate removal from aqueous solution. *Heliyon*, *8*(3), e09112. https://doi.org/10.1016/j.heliyon.2022.e09112

Salman, J. M., Abid, F. M., & Muhammed, A. A. (2012). Batch study for pesticide glyphosate adsorption onto palm oil fronds activated carbon. *Asian Journal of Chemistry*, *24*(12), 5646–5648.

Sen, K. (2021). A comprehensive review of glyphosate adsorption with factors influencing mechanism: Kinetics, isotherms, thermodynamics study. In *Intelligent environmental data monitoring for pollution management* (pp. 93–125). Elsevier.

Sen, K., Mondal, N. K., Chattoraj, S., & Datta, J. K. (2017). Statistical optimization study of adsorption parameters for the removal of glyphosate on forest soil using the response surface methodology. *Environmental Earth Sciences*, *76*, 22. https://doi.org/10.1007/s12665-016-6333-7

Van Bruggen, A. H. C., He, M. M., Shin, K., Mai, V., Jeong, K. C., Finckh, M. R., & Morris, J. G., Jr. (2018). Environmental and health effects of the herbicide glyphosate. *Science of the Total Environment*, *616–617*, 255–268.

World Health Organization. (2022). Chemical fact sheet: Glyphosate and AMPA. In *Guidelines for drinking-water quality: Fourth edition incorporating the first and second addenda*. World Health Organization.

©2026 This is an Open Access article distributed under the terms of the Creative Commons Attribution 4.0 International license viewed via https://creativecommons.org/licenses/by/4.0/ which permits unrestricted use, distribution, and reproduction in any medium, provided the original work is cited appropriately.